Ocean Engineering 267 (2023) 113180

Contents lists available at ScienceDirect

Ocean Engineering

journal homepage: www.elsevier.com/locate/oceaneng

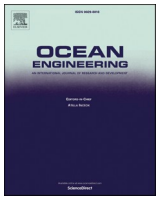

Determination of cyclic soil parameters for offshore foundation design from an existing data base

Knut H. Andersen [a,*], Harun Kursat Engin [a], Marco D'Ignazio [b,c], Shaoli Yang [a]

[a] Norwegian Geotechnical Institute, N-0855, Oslo, Norway
[b] Ramboll Finland Oy, Kansikatu 5B, 33100, Tampere, Finland
[c] Tampere Univ., Dept. of Civil Engrg., Faculty of Built Environment, Korkeakoulunkatu 5, 33720, Tampere, Finland

ARTICLE INFO

Keywords:
Offshore platforms
Cyclic loading
Wind
Waves
Soil parameters
Data base

ABSTRACT

Determination of the soil parameters in the foundation design analyses for offshore and nearshore platforms subjected to cyclic loading from wind and waves requires extensive advanced laboratory testing. The amount of such testing can be reduced by drawing on the experience that has been gained during the design of offshore structures in the past. It is outlined how an existing data base can be used to estimate the soil parameters needed in the foundation design analyses based on conventional parameters, like undrained static shear strength, plasticity index and overconsolidation ratio for clays, and relative density and/or water content, fines content and overconsolidation ratio for sand and silt. The estimated soil parameters can be used in feasibility analyses before site-specific parameters are available and to reduce the amount of site-specific advanced laboratory testing in the final design phase. The application of the data base is demonstrated by examples for clay and for sand with different fines content.

1. Introduction

Foundation design is an essential part of the design of offshore and nearshore fixed and floating platforms, both for wind turbines and for the continued development of oil and gas fields. The platforms are subjected to significant cyclic loading from wind and wave loading, and it is imperative for a safe and economical design to establish soil parameters that account for the effect of these cyclic loads.

Offshore platforms for oil and gas development have a more than 50-year-long history, with foundation design as an essential part. This has significantly contributed to geotechnical experience with soil investigation, laboratory testing, soil design parameters and design analyses. Prototype instrumentation and model testing have also provided considerable insight and learning. This experience from the oil and gas development is invaluable in the foundation design of future platforms, both offshore and nearshore.

The experience includes data bases with soil parameters that are required in the foundation design related to both capacity, displacements and dynamic behaviour. One such data base is the NGI data base related to the cyclic contour diagram concept and presented in several papers by e.g. Andersen (2004, 2015) and Andersen and Schjetne (2013). The data base covers different soil types, like clay, silt and sand with different plasticity, relative density, water content, particle size distribution and overconsolidation history. It includes shear strength, deformation and consolidation characteristics, for both monotonic and cyclic loading. The parameters are valid for different types of foundations, including skirted foundations, monopiles, gravity based, jack-ups, suction anchors and piles.

The parameters can be determined based on conventional soil properties and used for feasibility studies before site-specific data are available. The parameters may also be used in the final design, but then they should ideally be verified by some site-specific tests or used with great caution. Especially for wind parks with a large number of units and for nearshore conditions, the soil profiles can be very layered, and detailed testing of all layers may be prohibitive, also for the final design stage.

This paper will demonstrate how the data base mentioned above can be used to provide the soil parameters that are required for the foundation design of platforms under cyclic loading by means of examples for clay, silt and sand.

2. Foundation design aspects

The major requirements to be addressed in cyclic foundation design

* Corresponding author.
E-mail address: knut.h.andersen@ngi.no (K.H. Andersen).

https://doi.org/10.1016/j.oceaneng.2022.113180
Received 1 July 2022; Received in revised form 28 October 2022; Accepted 13 November 2022
Available online 14 December 2022

are: (1) ensuring sufficient bearing capacity; (2) making sure that cyclic displacements are tolerable; (3) providing equivalent soil spring stiffnesses and damping for use in dynamic soil-structure analyses; (4) assessing whether long term displacements due to permanent straining during cyclic loading are tolerable, (5) considering displacements developed during and after cycling through creep and pore pressure dissipation, and (6) assessing how soil reaction stresses developed at the soil-structure interface may change due to cycling. The importance of the different requirements depends on the type of foundation. The requirements are outlined and discussed in more detail by Andersen et al. (2013) and Andersen (2015).

3. Required soil parameters for foundation design

A number of soil parameters are required to address the design requirements. The influence of cyclic loading is especially important, and the data base described herein is related to the cyclic contour diagram concept (e.g. Andersen, 2015).

The soil parameters listed below may be required, but the list can be reduced for some foundation types and soil types.

- Cyclic shear strength
- Deformation parameters
- Pore pressure generation due to cyclic loading
- Initial shear modulus, G_{max}
- Consolidation characteristics (permeability, k and constrained modulus, M)
- Effective stress strength parameters, φ_p' and α'.
- Damping

The cyclic shear strength, deformation and pore pressure parameters depend on the average and cyclic shear stresses and the cyclic load history. A convenient way to express these parameters is in the form of contour diagrams where contours of number of cycles to failure, contours of average and cyclic shear strains and permanent pore pressure are plotted as functions of average and cyclic shear stresses for given number of cycles (e.g. N = 1, 10 and 100). The set of contours should also include cyclic shear strength, average and cyclic shear strains, and permanent pore pressure as functions of the number of cycles for a given average shear stress. Examples of contour diagrams are presented in the figures in Table 3. Andersen (2015) presents more examples and shows how the contour diagrams can be constructed and the laboratory testing that is required.

Both the shear strength and the deformation parameters are stress path dependent, and contour diagrams for both direct simple shear (DSS) and triaxial type of loading are required to take stress-path dependency into account. Stress-path dependency is referred to as anisotropy in this paper, without distinguishing between inherent and load-path induced anisotropies. As discussed later, anisotropy ratios may be used in simplified analyses if triaxial contour diagrams are not available.

Later sections show how site-specific parameters can be determined from the data bases for clay, silt and sand. The input parameters to the data base are vertical effective stress (σ'_{vc}), undrained shear strength (s_u), plasticity index (I_p) and overconsolidation ratio (OCR) for clays, and σ'_{vc}, relative density (D_r) and/or water content (w), fines content and OCR for sand and silt. A reference stress, σ'_{ref}, is used instead of σ'_{vc} in the data base since the normalized shear strength s_u/σ'_{ref} will be more independent of σ'_{vc} than s_u/σ'_{vc}. The reference stress is defined as $\sigma'_{ref} = p_a \cdot (\sigma'_{vc}/p_a)^n$, where p_a is the atmospheric pressure (=100 kPa), and n is a function of the normalized undrained static shear strength, s_u/σ'_{ref}, of the soil in its normally consolidated state. The n can be set to 0.9 for clays. Values of n for silt and sand are given in (Andersen, 2015).

The cyclic parameters should be based on cautiously estimated values of these input parameters, with the intention that they cover the uncertainties associated with the site- or location-specific soil profile.

The cyclic parameters are determined as best estimate values in the examples in this paper, and the correlations expressed as equations express best estimate values from the parameter plots. The uncertainties associated with establishing the best estimate values from the data base are beyond the scope of this paper. It is recommended to visit the diagrams in Andersen (2015) to see the scatter in the data to evaluate the uncertainty behind the equations. It is also recommended to visit Engin et al. (2021) who discuss uncertainties in design analyses, including uncertainties in the soil parameters and the consequences for the design analyses.

4. Available data

This paper mainly refers to the data base described in Andersen (2004, 2015) and Andersen and Schjetne (2013) and demonstrates how contour diagrams and other required design parameters can be determined as functions of conventional parameters and stress histories from this data base. The sand and silt parameters in the data base are generally based on silica soils with a coefficient of uniformity less than about $C_u = 12$ and $D_{60} < 0.2$ mm. The correlations may be less reliable for soils with other characteristics.

Additional data sets with cyclic contour diagrams for single, specific soils are available for clay (e.g. Andersen et al., 1988a,Andersen et al., 1988b, Andersen et al., 1989, Jeanjean et al., 1998, Kleven and Andersen, 1991, Andersen et al., 1993, Wichtmann et al., 2013, Liedtke et al., 2019, Liu et al., 2020a,b, He et al., 2021), sand and silt (e.g. Andersen and Berre, 1999; Yang et al., 2022; Blaker and Andersen, 2019) and calcareous soils (e.g. Finnie et al., 1999; Colreavy et al., 2022). The additional data sets give contour diagrams for one specific soil, however, and not as functions of conventional properties, and may not contain all the parameters that are needed. The information in the individual data sets prior to 2013 is also included in the general data base.

Damping is not part of the existing data base and is discussed in a separate section later in this paper.

5. Parameters for clay

The parameters needed to establish the cyclic parameters from the data base are the static DSS shear strength ratio (s_{uD}/σ'_{ref}), the plasticity index (I_p) and the overconsolidation ratio (OCR).

The following cyclic correlations are needed to perform a design:

- Number of cycles to failure, N_f, as a function of normalized average and cyclic shear stresses (τ_a/s_u and τ_{cy}/s_u)
- Cyclic and average shear strains (γ_a and γ_{cy}) as functions of normalized cyclic and average shear stresses (τ_a/s_u and τ_{cy}/s_u) for different number of cycles, e.g. N = 1, 10 and 100.
- Cyclic shear strain (γ_{cy}) as a function of normalized cyclic shear stress (τ_{cy}/s_u) and number of cycles (N) for $\tau_a = 0$.

These correlations are needed for DSS and triaxial stress paths and can be expressed in the form of contour diagrams. Examples can be seen in e.g. Andersen (2004). The contour diagrams will depend on OCR and I_p values. One may use a simplified approach where the contour diagrams are established for DSS type loading and empirical anisotropy factors are used to account for triaxial type stress paths. Anisotropy factors are discussed in a subsequent section.

The normalization of the contour diagrams is done with respect to the undrained static shear strength, since a representative undrained shear strength profile is normally established for clays. Normalization to σ'_{ref} can also be used, but the contour diagrams will then become very sensitive to OCR and may be more difficult to apply in practice (Andersen, 2015).

The correlations listed above are presented for Drammen Clay in Andersen (2004, 2015). The Drammen Clay data have often been found

to agree well with data from actual sites. The correlations are made more generally valid by including a correction factor for I_p different from Drammen Clay ($I_p = 27\%$).

The procedure to establish site-specific cyclic parameters can be done as explained in the following. The procedure is illustrated by two examples, Clay 1 and Clay 2, with different I_p and s_{uD}/σ'_{ref} as shown in Table 1. The correction factors are determined based on DSS tests, but these parameters shall also be applied for triaxial conditions.

1. Determine the equivalent OCR value for Drammen Clay based on the measured normalized static DSS strength (s_{uD}/σ'_{ref}) through the SHANSEP equation $(s_{uD}/\sigma'_{ref})_{OC}/(s_{uD}/\sigma'_{ref})_{NC} = OCR^m$ where $(s_{uD}/\sigma'_{ref})_{NC} = 0.21$ and $m = 0.78$, also presented graphically in Andersen (2004, 2015). This OCR should be in line with the measured OCR value if oedometer data is available.
2. Find the Drammen Clay DSS and triaxial contour diagrams for the OCR closest to the OCR determined in Step 1. The Drammen Clay data base contains contour diagrams for OCR of 1, 4 and 40 and can be found in Andersen (2004) and Andersen et al. (1988a, 1988b). The normalized cyclic shear strength at failure, $\tau_{f,cy}/s_u$, is not very sensitive to the OCR, but the average and cyclic shear strains depend strongly on OCR. Construction of new contour diagrams by interpolation between the diagrams may therefore be necessary if the site-specific OCR is not close to one of the Drammen Clay OCR values. Alternatively, the analyses can be done with contours for different OCR-values around the actual OCR and interpolating between derived stress strain curves or calculated displacements and calculated capacities afterwards.
3. Correct the contour diagrams for the effect of difference in I_p between the actual clay and Drammen Clay ($I_p = 27\%$) by the following factor that shall be applied on the vertical axis of the contour diagrams

$$F_{Ip} = (0.41 \cdot I_p^{0.224}) / (0.41 \cdot 27^{0.224}) \approx 0.48 \cdot I_p^{0.224}$$

The equation is based on the relationship between the normalized DSS cyclic shear strength at 10 cycles and I_p of $(\tau_{f,cy}/s_{uD})_{N\,=\,10} = 0.41 \cdot I_p^{0.224}$ (Andersen, 2015).

This scaling may give too low normalized stiffness for clays less plastic than Drammen Clay (i.e. $I_p<27\%$) and higher normalized stiffness for $I_p>27\%$. One should therefore consider adjusting for this. This can be done by adjusting the strain values on the strain contours in the contour diagrams, but it can be more convenient to perform this correction by adjusting the stress-strain curves derived from the contour diagrams or the calculated load-displacement curves. The adjustment is done by dividing the shear strains by a correction factor.

The adjustment at small strain or displacement level can be done based on the equation for the normalized initial shear modulus

$$(G_{max}/s_{uD}) = (30 + 300/(I_p/100 + 0.03)) \cdot OCR^{-0.25} \text{ (Andersen, 2015)}$$

Table 1
Cyclic shear strength and strain parameters for clay based on the data base in Andersen (2004, 2015).

Step:	Input		1	2	3	3	3
Unit	I_p (%)	s_{uD}/σ'_{ref}	OCR	Find contour diagram	Corr. factor for I_p on vertical axis. F_{Ip}	G_{max}/s_{uD} corr. factor for I_p. $F_{Ip\ small\ strain}$ [a]	G_{50}/s_{uD} corr. factor for I_p. $F_{Ip\ 50\%}$ [a]
Clay 1	27	0.62	4	Andersen (1988a &b, and 2004)	1.00	1.00	1.00
Clay 2	15	0.43	2.5		0.88	1.64	1.32

[a] Correction factor shall be applied by dividing the shear strain by the specified factor.

The correction relative to Drammen Clay ($I_p = 27\%$) will be independent of OCR and becomes

$$F_{Ip\ small\ strain} = 0.029 \cdot (1 + 10 \cdot (0.01 \cdot I_p + 0.03)^{-1})$$

The adjustment is expected to be smaller at higher shear stresses, and it is suggested to apply half the correction above at 50% of the failure load i.e. a correction factor of

$$F_{Ip\ 50\%} = 1 + (F_{Ip\ small\ strain} - 1)/2$$

The rest of the strain contours, the stress-strain curves or the load-displacement curves must be interpolated between the corrected values of failure shear stress, small strain stiffness and stiffness at half the failure load based on engineering judgement.

6. Parameters for sand and silt

The input parameters needed to establish the cyclic correlations from the data base are relative density (D_r) and/or water content (w), fines content (FC) and overconsolidation ratio (OCR).

The following cyclic correlations are needed to perform a design:

- Number of cycles to failure (N_f) as a function of average and cyclic shear stresses (τ_a/σ'_{ref} and τ_{cy}/σ'_{ref}) for drained and undrained values of $\Delta\tau_a = \tau_a - \tau_0$.
- Cyclic and average shear strains (γ_a and γ_{cy}) as functions of cyclic and average shear stresses (τ_a/σ'_{ref} and τ_{cy}/σ'_{ref}) for different number of cycles, e.g. N = 1, 10 and 100 for drained and undrained values of $\Delta\tau_a = \tau_a - \tau_0$.
- Cyclic shear strain (γ_{cy}) as a function of cyclic shear stress and number of cycles (N) for $\tau_a = 0$.
- Permanent pore pressure (u_p/σ'_{ref}) as a function of cyclic shear stress and number of cycles for $\tau_a = 0$.
- Consolidation characteristics, covering permeability and moduli for virgin loading, unloading and reloading conditions. The determination of consolidation characteristics is discussed separately in a later section.

Ideally, the cyclic correlations should be established for both DSS and triaxial conditions, but one may take a simplified approach to establish the contour diagrams for DSS type loading and use anisotropy factors to account for triaxial type stress paths. Anisotropy factors are discussed in a subsequent section.

A data base with cyclic correlations for sand and silt is presented in Andersen (2015). Examples for DSS conditions can be seen in Table 3. The correlations are given for a range of the input parameters, but the cyclic correlations may need adjustment to the exact site-specific conditions. The determination of the cyclic correlations can, with reference to Tables 2 and 3, be done by the steps explained in the following. Two examples for DSS conditions, Case A and Case B, with different D_r, w, FC and OCR as given in Table 2 are selected as illustrations. Both examples require scaling of the contour diagrams to be representative for the specified site-specific conditions. The examples follow and refer to the steps below.

1. Establish input parameters (D_r, w, FC and OCR)
2. Determine the normally consolidated undrained static DSS shear strength (τ_f/σ'_{ref}) by entering the diagram for undrained static shear strength with D_r and FC. The strength can also be determined from a similar diagram with water content as input instead of D_r. This can give a valuable supplement to determination based on D_r.
3. Determine the normally consolidated undrained cyclic DSS shear strength for N = 10 at $\tau_a = 0$ $(\tau_{cy,f}/\sigma'_{ref})_{N\,=\,10}$, by entering the cyclic shear strength diagram with D_r and FC. The cyclic strength can also be determined from a diagram with w as input instead of D_r, as for the static shear strength.

Table 2
Cyclic soil parameters for example cases A and B.

$\Delta\tau_a$ Drainage condition	w	D_r	Fines content	OCR	τ_f/σ_{ref}' static	$\tau_{cy,f}/\sigma_{ref}'$ cyclic N = 10	α' (^{0})	tan α'	OCR corr.	τ_f/σ_{ref}' static	n static	$\tau_{cy,f}/\sigma_{ref}'$ N = 10	Contour			G correction factor [2]	
	%	%	(%)		DSS OCR = 1		at 100 kPa		factor	DSS with OCR corr.			Diagram Type [1]	Factor static	Factor cyclic	G_{max}/τ_f	G_{50}/τ_f
Step:	*1*	*1*	*1*	*1*	*2*	*3*	*4*	*4*	*5*	*5*	*5*	*5*	*6*	*7*	*7*	*8*	*8*
Case A																	
Undrained	26	70	20	2	0.3	0.17			1.62	0.49	0.9	0.28	Undrained B	1.00	1.12	0.86	0.68
Drained	26	70	20	2	0.3	0.17	37.7	0.77	1.62			0.28	Drained B	1.04	1.12	0.86	0.68
Case B																	
Undrained	22	90	10	6	3.5	0.46			1.24	4.34	0.4	0.57	Undrained C	1.09	0.95	0.93	0.84
Drained	22	90	10	6	3.5	0.46	41.9	0.90	1.24			0.57	Drained C	1.08	0.95	0.93	0.84

[1] Diagram Type refers diagrams in Figs 12.15, 12.16, 13.1, 13.2–13.11 & 14.1 in Andersen (2015).
[2] G/τ_f correction factor shall be 1.0 for γ_a in the drained case.

4. Determine the slope of the failure line (α′) in the effective stress path for drained DSS tests. Andersen (2015) presented plots of α′ vs. D_r and water content. The slope for a consolidation stress of $\sigma'_{vc} = 100$ kPa in this diagram can be expressed as a function of relative density by

$$\alpha'_{100} = 0.21 \cdot D_r + 23$$

or as function of water content by

$$\alpha'_{100} = 70\text{-}1.3 \cdot w$$

The slope for an arbitrary consolidation stress, σ'_{vc}, can be determined from

$$\alpha'_{\sigma'vc}/\alpha'_{100} = 3 \cdot 10^{-6} \cdot \sigma'^2_{vc} - 0.0023 \cdot \sigma'_{vc} + 1.21$$

The α′−value to be used in the following is the value for a consolidation stress of $\sigma'_{vc} = 100$ kPa because this will be consistent with normalization to σ'_{ref} ($\sigma'_{ref} = \sigma'_{vc}$ for $\sigma'_{vc} = 100$ kPa).

5. Determine the OCR correction factor. The values determined in the previous steps are for normally consolidated soils. The OCR correction depends on whether the soil contracts or dilates in the normally consolidated state. The normalized undrained static DSS strength, $(\tau_f/\sigma'_{ref})_{NC}$, is used to evaluate this. A low normally consolidated τ_f/σ'_{ref} indicates a strongly contracting soil, like a clay or a loose sand or silt, and the undrained shear strength will be strongly influenced by OCR. A high normally consolidated τ_f/σ'_{ref} indicates a strongly dilatant soil, like a very dense sand or silt, and will be marginally influenced by OCR.
Andersen (2015) presented a plot of the ratio between the normalized undrained shear strengths of overconsolidated and normally consolidated soils that can be estimated by the following expressions:

$$(\tau_f/\sigma'_{ref})_{OC} / (\tau_f/\sigma'_{ref})_{NC} = OCR^m$$

where

$m = 0.78$ for clay

$m = 1.13\text{–}1.45 \cdot (\tau_f/\sigma'_{ref})_{NC}$ with $m_{max} = 0.8$ for sand/silt when $(\tau_f/\sigma'_{ref})_{NC} < 0.44$

$m = 0.54\text{–}0.12 \cdot (\tau_f/\sigma'_{ref})_{NC}$ with $m_{min} = 0$ for sand/silt when $(\tau_f/\sigma'_{ref})_{NC} > 0.44$

The OCR correction shall be applied on both cyclic and static undrained shear strengths. In the case of drained average shear stress, however, the OCR correction can be applied on the cyclic shear stress, but the OCR correction shall not be applied on the part of the failure curve where the failure mode is governed by large average shear strain or on the average shear strain contours (Andersen, 2015).

6. The contour diagrams depend on the drainage conditions during the storm. The contour diagrams assume undrained conditions within each cycle, but the average shear stress can be drained or undrained, and diagrams for both drained and undrained average shear stress may be required. The drainage under average shear stress can be calculated when the variation of the average load during the peak part of the storm is known. Both drained and undrained static shear stress conditions are presented in Tables 2 and 3 The effect of drainage under the average shear stress can be significant. Comparison between the static shear strengths shows whether drained or undrained average shear stress condition will be critical. One may choose to use the most conservative in cases where drainage is uncertain.
It is important to check that the assumption of undrained conditions under a single cycle is valid, especially for dense sand where the effective stress due to dilatancy can be lost if drainage occurs.
7. When the cyclic and static shear strengths are established, the cyclic parameters are established by determining scaling factors to the cyclic contour diagram with the static and cyclic shear strengths closest to the cyclic and static shear strengths established above. The scaling factors are given for both drained and undrained average shear stress ($\Delta\tau_a$) conditions. The scaling factors for the data base refer to the diagrams in Figures 12.15, 12.16, 13.1 to 13.11 and 14.1 in Andersen (2015), each subnumbered by letter a to e in alphabetic order from the top. Scaling from a diagram with a higher cyclic strength will give stiffnesses on the low side, whereas scaling from a diagram with lower cyclic shear strength will give stiffnesses on the high side.
8. The contours in the diagrams in the data base are for normally consolidated sands and silts. The normalized shear stiffness will decrease with increasing OCR, and the strain or stiffnesses based on these contours should be corrected if they are used for overconsolidated soils. Andersen (2015) presented a plot of the ratio between the normalized shear stiffnesses of overconsolidated and normally consolidated soils. The ratio is higher for the small strain modulus than for the modulus at shear stress levels above 20% shear strength mobilization. The ratios can be estimated by the following expressions:

$$(G_{max}/\tau_f)_{OC} / (G_{max}/\tau_f)_{NC} = OCR^{-p} \text{ where } p = 0.32 \cdot m$$

Table 3
Example cases A and B. Figures are simplified versions of figures in Andersen (2015).

	Case A	Case B
Step 1	Establish input parameters (D_r, w, FC, OCR)	
Step 2	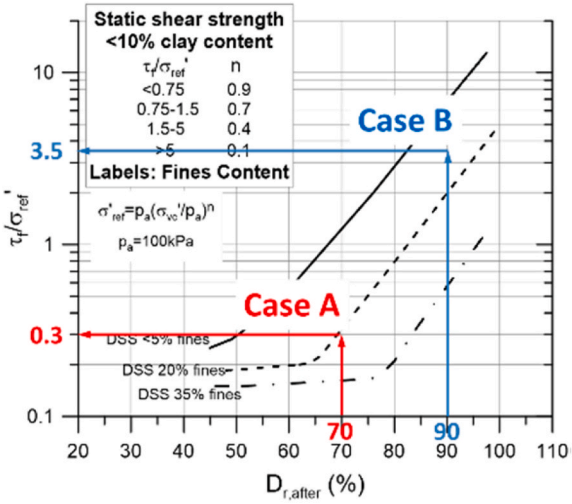	
Step 3	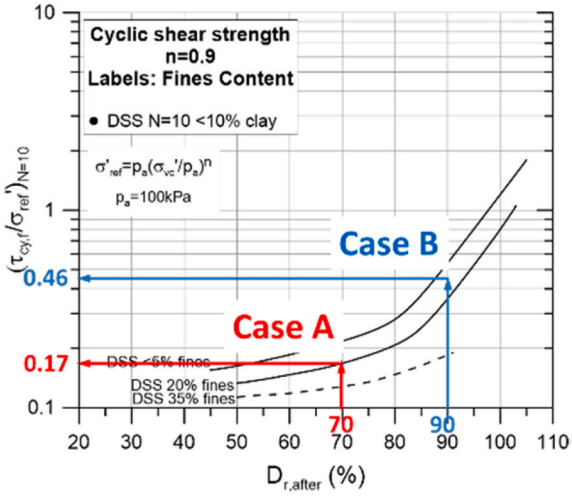	
Step 4	$\alpha'_{100} = 0.21 \cdot D_r + 23$ or $\alpha'_{100} = 70\text{-}1.3 \cdot w$	
Step 5	$(\tau_f/\sigma'_{ref})_{OC}/(\tau_f/\sigma'_{ref})_{NC} = OCR^m$	
Step 6/7	Failure contours. Undrained $\Delta\tau_a$	
	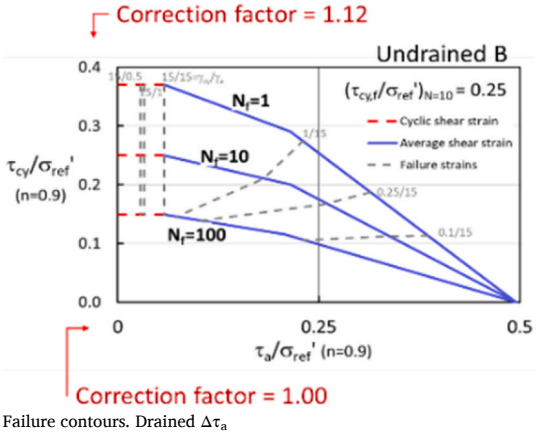	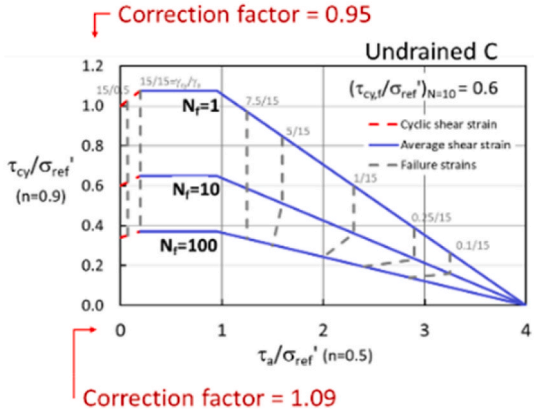
	Failure contours. Drained $\Delta\tau_a$	

(*continued on next page*)

Table 3 (*continued*)

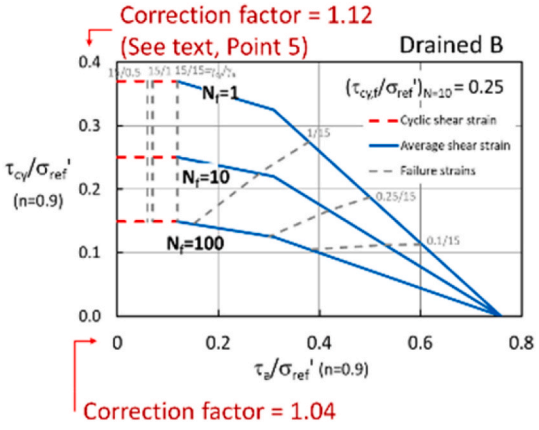

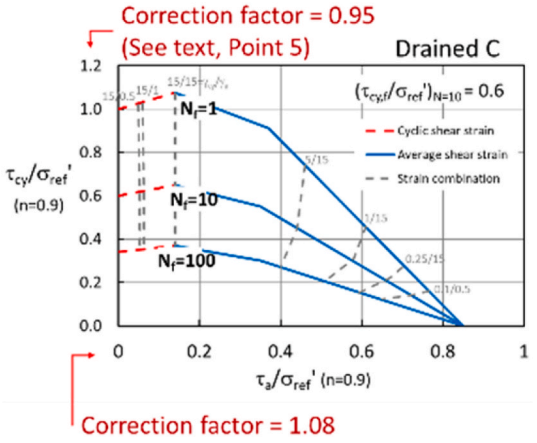

Cyclic shear strain = f (log N, τ_{cy}/σ_{ref}') for $\Delta\tau_a = 0$

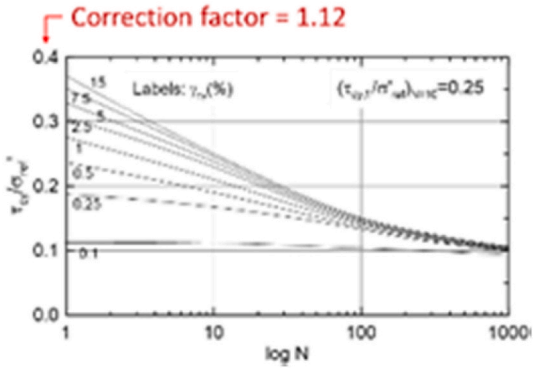

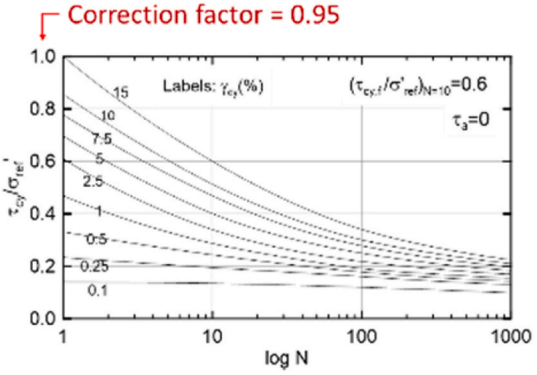

u_p/σ_{ref}' = f (log N, τ_{cy}/σ_{ref}') for $\Delta\tau_a = 0$

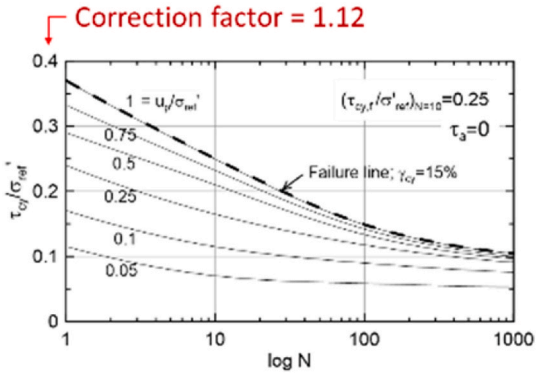

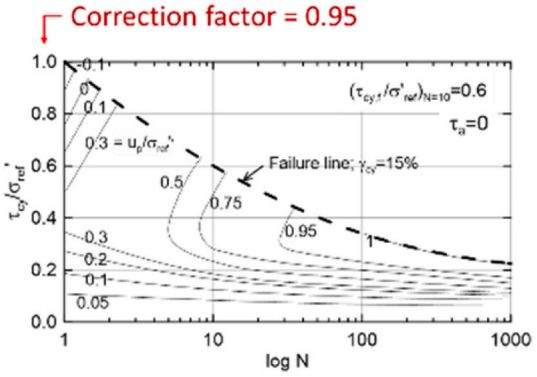

γ_a and γ_{cy} = f (τ_a/σ_{ref}', τ_{cy}/σ_{ref}') for N = 10. Undrained $\Delta\tau_a$

(*continued on next page*)

Table 3 (*continued*)

	γ_a and $\gamma_{cy} = f(\tau_a/\sigma_{ref}', \tau_{cy}/\sigma_{ref}')$ for N = 10. Drained $\Delta\tau_a$	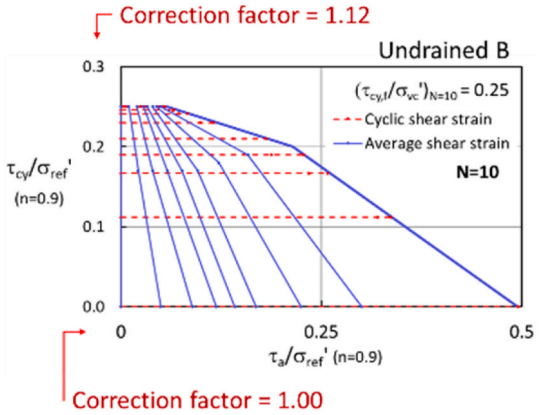 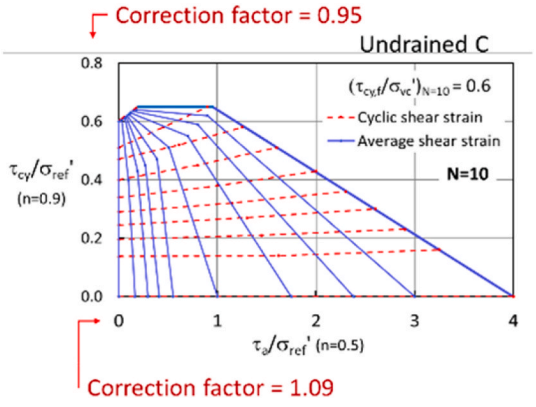
		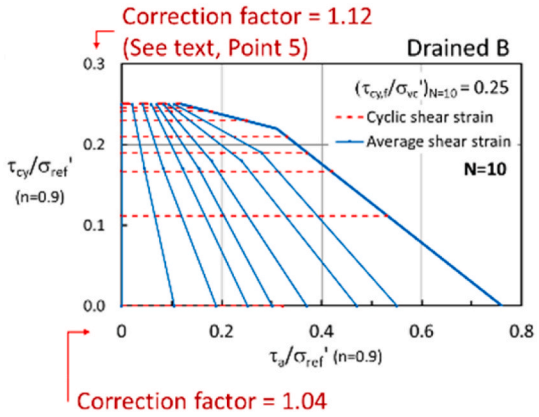 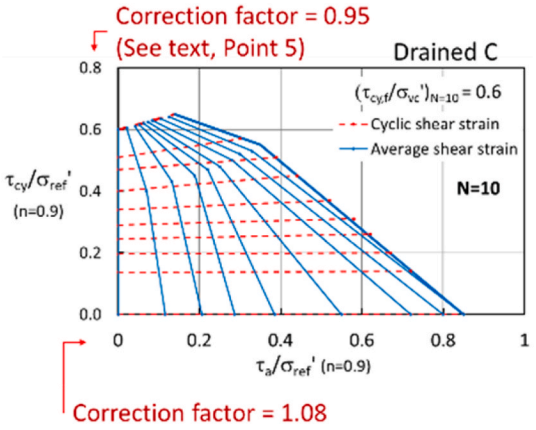
Step 8	$(G/s_{uD})_{OC}/(G/s_{uD})_{NC} = OCR^{-p}$	

$(G_{50}/\tau_f)_{OC}/(G_{50}/\tau_f)_{NC} = OCR^{-p}$ where $p = 0.8 \cdot m$

where m is defined in Step 5 above and τ_f is the undrained static DSS shear strength.

G_{max} is representative for the small strain behaviour, whereas G_{50} is believed to be the best representation for the serviceability stiffness and the displacements under the maximum loads.

It may be most practical to apply the corrections on the stress strain curves derived from the contour diagrams or on the calculated displacements, rather than correcting the strain contours in the diagrams.

7. Anisotropy

7.1. Strength anisotropy ratios

The cyclic shear strength is defined as $\tau_{f,cy}/s_u = \tau_{a,f}/s_u + \tau_{cy,f}/s_u$, where $\tau_{f,cy}/s_u$ is the normalized cyclic shear strength. $\tau_{a,f}/s_u$ and $\tau_{cy,f}/s_u$ are the average and cyclic shear stress components at failure, respectively (Fig. 1). The cyclic shear strength will depend on (1) the cyclic load history, (2) the ratio between cyclic and average shear stresses, (3) the stress path (i.e. DSS vs. triaxial type of element), and (4) drainage under the average load ($\Delta\tau_a$).

The cyclic load history can be transformed into an equivalent number of cycles, N_{eq}, which is the number of cycles of the maximum cyclic load that gives the same effect as the actual load history. N_{eq} can be determined by the strain or the pore pressure accumulation procedure (e.g. Andersen, 2015). The N_{eq} determination can be done separately for DSS and triaxial conditions, but accumulation is often done in the contour diagram for DSS tests with symmetrical loading ($\tau_a = 0$) in simplistic practical calculations.

The ratio between the cyclic and the average shear stresses will depend on the weight of the structure and the ratio between the cyclic and average components in the load history. The simplest approach is to assume that the ratio between the cyclic and average shear stresses in the soil are $\tau_{cy}/(\tau_a-\tau_0) = P_{cy}/P_a$, where τ_0 is the initial shear stress in the soil, and P are the loads from the platform to the soil. A clay will normally not be consolidated under the platform weight prior to the design event, and τ_0 will then be due to the soil overburden. A sand may be consolidated, and the weight should then be included in the τ_0 calculation for the soil beneath the platform.

The assumption of a constant $\tau_{cy}/(\tau_a-\tau_0)$ will give the stress paths indicated by the full line in the DSS diagram and the dotted lines in the triaxial diagrams in Fig. 1. The example assumes a ratio of $\tau_{cy}/(\tau_a-\tau_0) = 1$. Inspection of the shear strain combination where the different paths intersect the failure envelope will usually show that the average and cyclic shear strains at failure are very different in the DSS and the triaxial contours and that there will not be strain compatibility along a failure surface that involves compression, DSS and extension type elements. In order to achieve strain compatibility, both average and cyclic shear stresses need to be redistributed, and the stress paths will look more like the fully drawn curves in Fig. 1. It can be discussed whether full strain compatibility will occur, but with that assumption, the cyclic shear strength can be defined. The example assumes DSS failure mode to be dominating, but the same exercise can be done with other assumptions. The cyclic shear strength for the different stress paths is defined by the intersection between the load path and the failure envelope.

This procedure requires both DSS and triaxial contour diagrams. The data bases normally contain more DSS than triaxial type contours, and examples of anisotropy ratios that one may apply as approximations in lieu of triaxial contours are presented in Tables 4 and 5. The tables

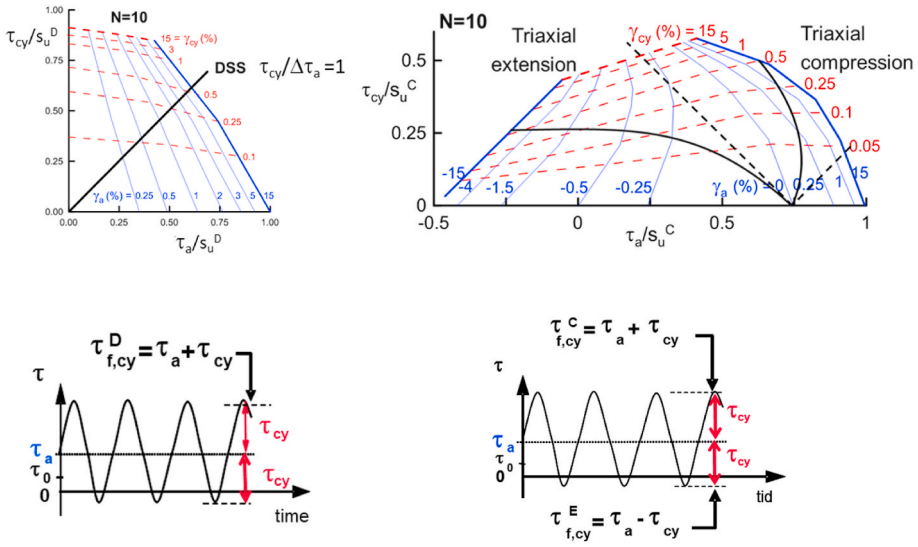

Fig. 1. Definition of cyclic shear strength and illustration of stress paths accounting for stress redistribution to achieve strain compatibility. Based on Andersen (2015).

Table 4
Approximate anisotropy ratios for clay (undrained).

Loading	OCR	CAUC/DSS		CAUE/DSS		Comments
		Total	Cyclic	Total	Cyclic	
Static	–	1.25[a]-1.45[b]	–	0.78[a]-0.61[b]	–	Lunne and Andersen (2007)
	1–40	1.45	–	0.78	–	Drammen, Andersen (2004)
Cyclic	1	1.25	1	0.5	0.65	Drammen, Andersen (2004)
	4	1.25	1	0.75	1	
	40	1	1	0.75	1	All $\tau_{cy}/\Delta\tau_a$

[a] Offshore samples.
[b] High quality samples.

contain both static and cyclic anisotropy ratios. The cyclic anisotropy ratios have been developed for soils where both DSS and triaxial contours have been available. The strength anisotropy ratios are generally conservative (low) best estimate values but can also be on the optimistic side in a few cases.

The static strength anisotropy ratios for clay in Table 4 are based on experience from onshore and offshore soil investigations (Lunne and Andersen, 2007) and Drammen Clay (e.g. Andersen, 2004). The cyclic shear strength anisotropy ratios are based on contour diagrams for Drammen Clay (e.g. Andersen, 2004) and are valid over the full range of $\tau_{cy}/(\tau_a-\tau_0)$ ratios. They are developed for N = 10, but are reasonably independent of N.

The static and cyclic shear strength anisotropy ratios for sand and silt are based on Andersen (2015), supplemented with data from Dogger

Table 5
Approximate anisotropy ratios for sand (U means $\Delta\tau_a$ applied undrained. D+ means $\Delta\tau_a$ applied drained by increasing the normal stress. D-means $\Delta\tau_a$ applied drained by decreasing the normal stress).

Loading	D_r (%)	Drainage	CAUC/DSS		CAUE/DSS		Comments
			Total	Cyclic	Total	Cyclic	
Static	≥80%	U	4	–	1.1	–	Andersen (2015) Fig 10.4b.
	70–80%	U	3	–	1	–	
	60–70%	U	2	–	0.7	–	
	<60%	U	1.45	–	0.7	–	
	All D_r	D+	1[a] - 2.25[b]	–	2.25	–	
	All D_r	D-	0.45	–	0.2[a] - 0.45[b]	–	Drained based on formulas and α′ in Andersen (2015). φ′ from Andersen and Schjetne (2012).
Cyclic	≥80%	U	2[c] (1.6–2.3)[d]	–	1.35[c] (0.6–2)[d]	–	Fig 12.1 Andersen (2015).
	≥80%	D+	2.5[c] (2–3.5)[d]	2.7	1.5[c] (1–1.8)[d]	–	
	≥80%	D-	1.5[c] (1.1–1.8)[d]	–	0.6[c] (0.4–0.75)[d]	1.5	
	80 - 60%	U, D+, D-	[e]	–	[e]	–	
	<60%	U	1.25	1	0.5	0.65	D_r < 80% is especially uncertain; must be used with great care!
		D+	–	–	–	–	
		D-	–	–	–	–	

[a] K_0' = 0.5.
[b] K_0' = 1.0.
[c] Best estimate.
[d] Range.
[e] Scale linearly between 80% and 60%.

Bank (Blaker and Andersen, 2015) and experience from actual projects. It is necessary to determine whether there can be drainage under the average shear stress ($\Delta\tau_a$) in sand and silt since this will decide what type of contour diagram that shall be used. Examples showing the effect drainage can have on the contour diagrams are presented in Figs. 2 and 3. It is important to note that the drained static triaxial shear strength depends strongly on whether the average shear stress ($\Delta\tau_a = 0.5\cdot(\Delta\sigma_v\text{-}\Delta\sigma_h)$) is applied by increasing or decreasing the normal stress. The static shear strength defines the intersection point at the horizontal axis and has a governing influence on the contours. Fig. 3b shows the contours for the case where the drained $\Delta\tau_a$ is applied by changing the vertical normal stress. The intersection points of the contours at the horizontal axis for the case with changing horizontal normal stress are also indicated. The contours for the case with drained change in horizontal normal stress need to be consistent with these intersection points. Examples are shown in Andersen (2015). The DSS examples in Fig. 2 show that drained conditions generally give lower shear strengths than undrained for very dense sand. The opposite will be the case for low density.

The undrained static strength ratios for sand and silt in Table 5 can be established from Figure 10.4b in Andersen (2015). The static strength anisotropy ratios for drained conditions can be established using the strength formula for the different stress paths (Andersen, 2015) with values of α' and φ' as functions of relative density according to the equations in Sections 6 and 10, respectively.

Tables 4 and 5 show that there can be significant differences between the triaxial compression (s_{uC}), DSS (s_{uD}) and triaxial extension (s_{uE}) strengths, for both static and cyclic loading. In many cases, the DSS strength can be a reasonable first estimate of the average strength, but this requires that the three strengths contribute equally much to the capacity. The triaxial compression strength can be significantly higher than the DSS strength in dense sand and silt, and the triaxial extension strength can also be higher than the DSS strength. This can have a significant influence on the failure mechanism and the capacity and stiffness of a foundation. Therefore, anisotropy should be given attention in design. The capacity and stiffnesses of structures on dense sands and silts can be significantly underestimated if the design is based on DSS strength without consideration of anisotropy.

7.2. Stress-strain anisotropy ratios

The anisotropy factors described above can be applied in limiting equilibrium analyses and in finite element analyses where the cyclic shear strengths for triaxial compression, DSS and triaxial extension are given as input (e.g. Andersen and Jostad, 1999; Andersen et al., 2005; Jostad and Andersen, 2015).

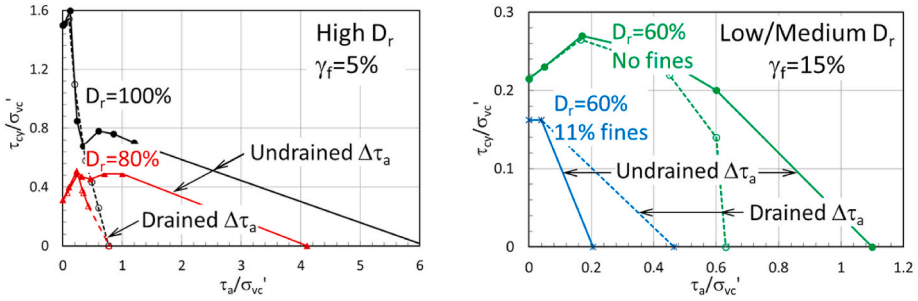

Fig. 2. Comparison of contours for $N_f = 10$ in DSS tests for undrained and drained conditions (based on Andersen, 2015).

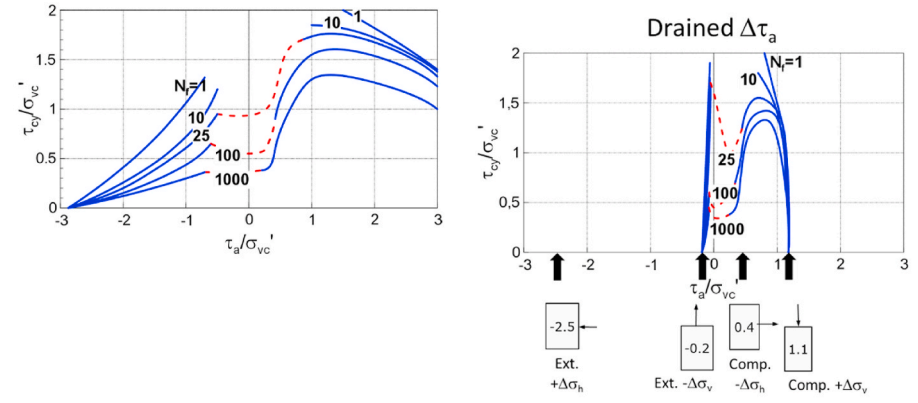

a) Undrained $\Delta\tau_a$

b) Drained $\Delta\tau_a$. Curves are for case where $\Delta\tau_a$ is applied by changing σ_v. Intersection points at horizontal axis for case where $\Delta\tau_a$ is applied by changing σ_h are also indicated.

Fig. 3. Example of difference in triaxial contour diagrams between undrained and drained $\Delta\tau_a$ conditions for very dense sand (based on Andersen, 2015).

Finite element analyses to calculate displacements and stiffnesses require stress-strain input in addition to shear strength. The stress-strain curves can be established by reading corresponding values of shear stress and shear strain along the curves in Fig. 1. This can be done separately for cyclic and average components (τ_{cy} vs. γ_{cy} and τ_a vs. γ_a). The average and cyclic components can be added to establish curves for ($\tau_a+\tau_{cy}$) vs. ($\gamma_a+\gamma_{cy}$) if one wants to calculate maximum displacements under maximum load. Ideally, anisotropy should be accounted for by using different curves for DSS, triaxial compression and triaxial extension. Examples of stress-strain curves derived from the contour diagrams as described above are given in Andersen (2015) and Engin et al. (2021).

A simpler, but more approximate approach is to use the strength anisotropy factors to scale the DSS stress-strain curves. Examples of anisotropy ratios as functions of shear strain are shown for different sands with a load path ratio of 1.5 and N = 10 in Fig. 4. The figures show that the anisotropy ratio tends to decrease with increasing shear strain. Using the anisotropy ratio at failure for the whole stress-strain curve may thus underestimate the stiffness at stresses below failure. It is important to note, however, that the stress-strain curves may have significantly different shapes in DSS, triaxial compression and triaxial extension, especially for the average components, which show differences similar to what is observed in monotonic tests (e.g. Andersen, 2015).

7.3. Alternative methods

In more sophisticated analyses, the cyclic shear strengths and shear strains are determined as part of the analysis. These alternatives require input in the form of contour diagrams for both DSS and triaxial tests.

Andersen and Lauritzsen (1988a) proposed a limiting equilibrium approach where the shear stress redistribution is accounted for. The method is based on the assumption that the combination of average and cyclic shear strains is the same along the potential failure surface (strain compatibility), and on the condition that the average shear stress along the potential failure surface is in equilibrium with the average loads. The critical γ_{cy}/γ_a combination can be determined by iteration.

The most advanced alternative is to use a finite element code where the stress path is calculated in each integration point and the stress-strain characteristics are defined by input in the form of contour diagrams. Such finite element codes (UDCAM and PDCAM) are described by Jostad et al. (2014, 2015). The strain or pore pressure accumulation is also taken care of in the codes. UDCAM is developed for undrained conditions, whereas PDCAM can account for the drainage and pore pressure redistribution that can occur during the cyclic load history. The $\tau_{cy}/(\tau_a-\tau_0)$-ratio can vary from one integration point to the next in these codes.

8. Initial shear modulus

The initial shear modulus may be required to calculate the foundation stiffness under small loads. The initial shear modulus can be used to supplement the contour diagrams with contours for smaller strains than those in the existing diagrams or to adjust the initial part of stress-strain curves derived from the contour diagrams.

The initial shear modulus for clays can be calculated by the expressions (Andersen, 2015)

$$G_{max}/s_{uD} = (30 + 300/(I_p/100 + 0.03))\cdot OCR^{-0.25}$$

or

$$G_{max}/\sigma'_{ref} = (30 + 75/(I_p/100 + 0.03))\cdot OCR^{0.5}$$

There are several formulas that express the initial shear modulus for sand based on void ratio and mean effective stress, like the one from Hardin and Drnevich (1972):

$$G_{max}/\sigma'^{0.5}_{oct} = 3222\cdot(3\text{-}e)^2/(1+e) \text{ (parameters in kPa)}$$

9. Consolidation characteristics

The consolidation characteristics are needed to calculate pore pressure dissipation, effective stress changes and settlements due to the

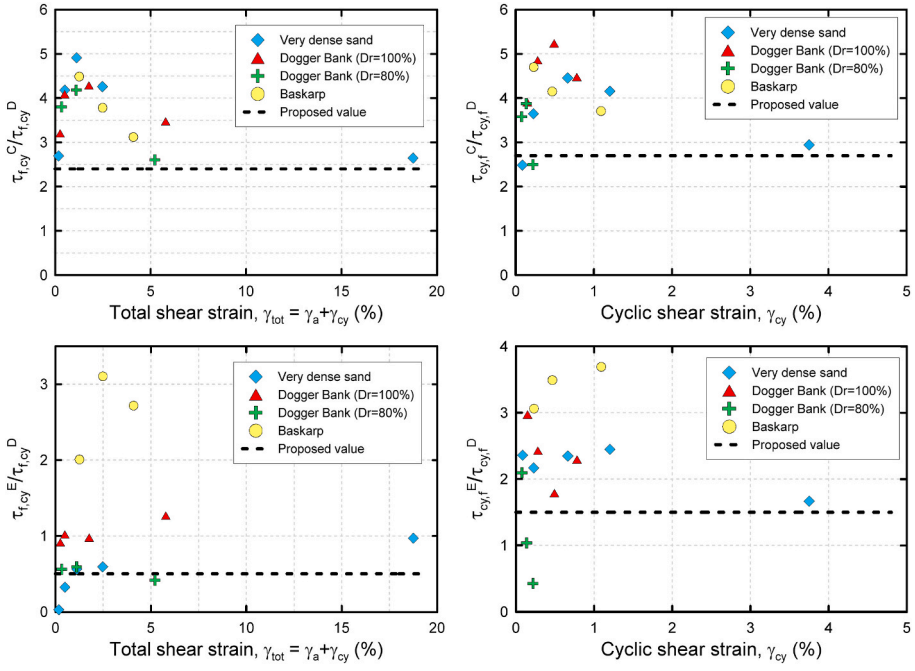

a) Total stress-strain behaviour *b) Cyclic stress-strain behaviour*

Fig. 4. Anisotropy ratio for stress-strain behaviour. Various sands with load path ratio of $\tau_{cy}/\tau_a = 1.5$ and N = 10. Compression/DSS (upper), extension/DSS (lower).

platform weight, dissipation of pore pressure during the cyclic load history, and to check that the conditions are undrained during individual cycles. Such calculations require consolidation characteristics in the form of permeability coefficient and modulus. The modulus may be needed for both virgin loading, unloading and reloading, depending on the project.

The coefficient of permeability and the moduli can be estimated from data bases based on water content (or void ratio), fines content, clay content and D_{10}. A data base for permeability can be found in Andersen and Schjetne (2013), which also gives the framework for moduli under both virgin loading, unloading and reloading. The latest parameter correlations for this moduli framework are given in Andersen (2015).

10. Friction angle

It is most convenient to use the φ_p' and α' at a consolidation stress of 100 kPa to determine the drained strengths to apply when constructing contour diagrams. The strengths will then be consistent with normalization to σ'_{ref} since $\sigma'_{ref} = \sigma'_{vc}$ when $\sigma'_{vc} = 100$ kPa. The effect of σ'_{vc} will then be accounted for in normalization to σ'_{ref}.

The correlation of φ_p' and α' with D_r can be expressed as

$$\varphi_p' = 32.4 + 0.077 \cdot D_r + 0.00036 \cdot D_r^2 \text{ (for } \sigma'_{vc} = 100\text{–}199 \text{ kPa)}$$

$$\alpha'_{100} = 0.21 \cdot D_r + 23 \text{ or } \alpha'_{100} = 70\text{-}1.3 \cdot w \text{ for } \sigma'_{vc} = 100 \text{ kPa}$$

The drained peak friction angle is also required to calculate e.g. the skirt penetration resistance by the bearing capacity approach. The empirical constants in Andersen et al. (2008) are based on φ_p' at σ'_{vc} = 100–250 kPa. The equation above is thus also applicable for skirt penetration resistance.

11. Damping

Damping in the soil has not been an important issue in the foundation design of offshore platforms so far. Soil damping parameters have therefore not received the same attention as strength and moduli and are not part of the database in Andersen (2015). Soil damping can be more important for wind power foundations, due to different cyclic load characteristics and platform design. Soil damping information may therefore need to be considered. Rather than developing contour diagrams for damping, however, it seems more practical to relate the damping ratio (D) to γ_{cy}, which is the way it has been expressed in the literature. In the approach proposed in this paper, D can then be related to the γ_{cy} determined as described in previous sections.

11.1. Literature

Several authors have published empirical correlations expressing damping, D, as a function of γ_{cy}. One of the early references which has been widely used, especially in earthquake engineering, is Seed and Idriss (1970) who present separate correlations for sand and clay. Seed and Idriss (1970) partly drew upon a contemporary study by Hardin and Drnevich (1970).

Seed et al. (1986) reinterpreted the Seed and Idriss (1970) curves and confirmed the damping curves for sand. Sun et al. (1988) developed a correlation for clay which was in agreement with Seed and Idriss (1970). Idriss (1990) presented a common curve for sand and clay similar to Seed and Idriss (1970) for clay, which is lower than Seed and Idriss (1970) for sand.

More recently, Vucetic and Dobry (1991) and Darendeli (2001) have published correlations for sand and clay with I_p as an important parameter.

Darendeli (2001) rates the importance of different parameters and states that.

- effective stress, soil type, plasticity and number of cycles can be very important
- load period can be important
- OCR, void ratio, and grain characteristics, size, shape, gradation and mineralogy can be less important
- fines content is not important

However, the Darendeli (2001) formulas do not always seem to support this ranking.

Vucetic and Dobry (1991) state that the I_p is the most important parameter, and that there is little influence of test type, OCR and N. They found a relatively large variation in D_{min} of 1%–5.5% with no clear relation to I_p, however.

Seed and Idriss (1970) state that the effect of number of cycles is small and that the effect of consolidation stress is important for sand.

The correlations above are generally valid for symmetrical cyclic loading with $N \leq 10$ at a load period of 1s on normally consolidated soils. None of the references give guidance for non-symmetrical cyclic loading.

11.2. NGI tests

NGI has interpreted damping from cyclic DSS, triaxial and resonant column laboratory tests on clay and cyclic DSS and triaxial laboratory tests on dense sand (e.g. Blaker and Andersen, 2019; Løvholt et al., 2020). The cyclic loading was applied load controlled with a load period of 10s for most tests. The damping ratio was derived by using an improved method for interpretation of the damping, taking the influence of permanent strain accumulation into account (Løvholt et al., 2020).

The tests on clay were run on intact samples with OCR in the range 1.35–1.5 of high, medium and low plasticity with I_p of about 80%, 37% and 18%, respectively as well as on a quick clay.

The tests on sand were run on two batches of fine to medium Dogger Bank sand (Blaker and Andersen, 2019). Batch A had essentially no fines, and Batch B had 20% fines. Triaxial and DSS tests were run on two relative densities, D_r = 80% and 100%, in a normally consolidated state. The D_r = 80% specimens from Batch A were also tested at OCR = 4.

11.3. Comparisons

The different correlations are plotted for high plasticity clay, low plasticity clay, sand with 20% fines, and clean sand, in Figs. 5 and 6. The results from the NGI tests are included, both as results from individual tests and as contours based on the tests. The illustration of the effect of parameters like OCR, τ_a, load period, σ'_{vc} and triaxial vs. DSS in the NGI tests is limited due to space limitations.

Comparison of the correlations show similarities, but also considerable differences in some cases. The agreement between the NGI tests and the correlations depends on the soil. Some main findings are listed below.

General:

- The range between the upper and lower Seed and Idriss (1970) curves is very wide. It would be very conservative to use the most unfavourable limit in some cases.
- The correlations show that N has a small effect on D. This does not agree with the NGI tests, as discussed below. The effect of N is important to note especially for fatigue analyses where the number of representative cycles can be high.
- Seed and Idriss (1970) mean curve, Vucetic and Dobry (1991) and Darendeli (2001) give similar D for clay with I_p = 15%–30%, but the effect of I_p is much more significant in Vucetic and Dobry (1991) which gives lower D than the two other at high I_p. Seed and Idriss (1970) is independent of I_p.
- The correlations do not discuss the effect of τ_a. The NGI tests show that D increases with increasing average shear stress in the clays, and it will be conservative (low D) to use D from DSS tests with

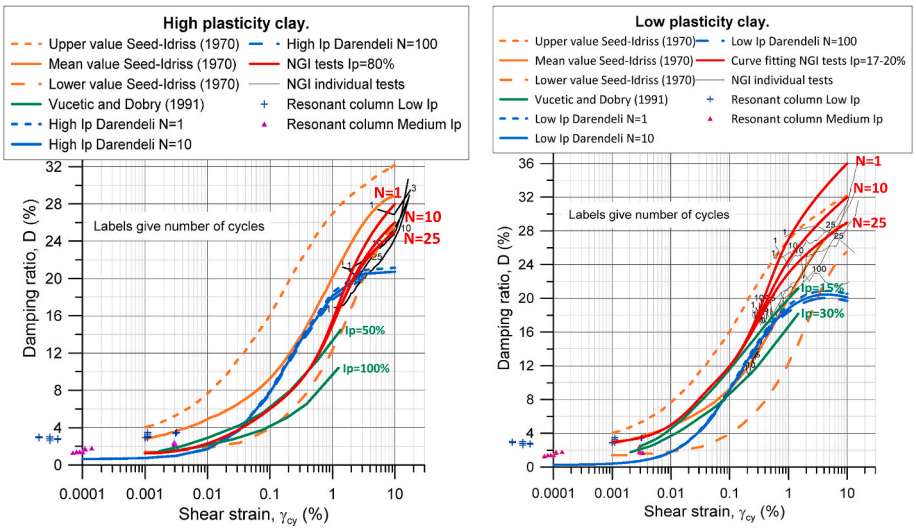

Fig. 5. Empirical correlations of D with γ_{cy} from literature and results from NGI tests for high and low plasticity clays.

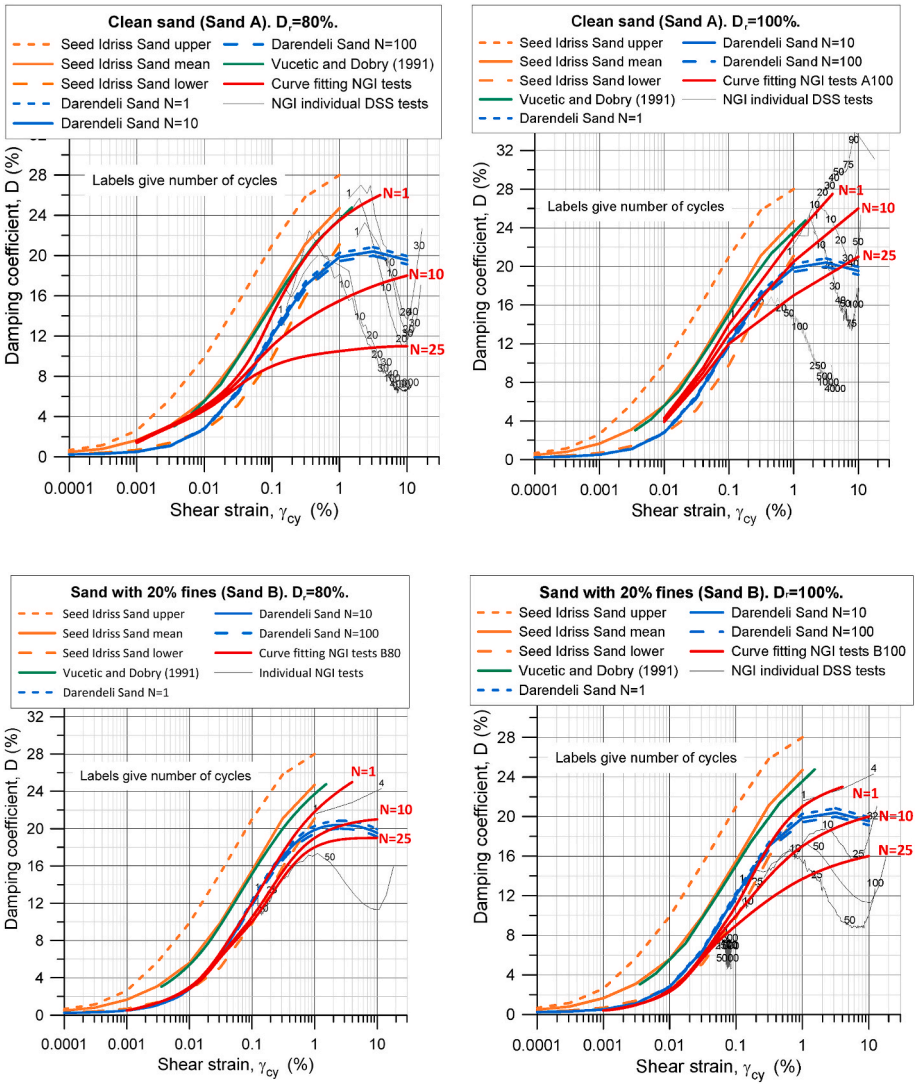

Fig. 6. Empirical correlations of D with γ_{cy} from literature and results from NGI tests for clean sand and sand with FC = 20% at D_r = 80% and 100%.

symmetrical cyclic loading. The effect is less conclusive in the dense sand.
- D tends to increase with increasing load period.
- Correlations for sand give higher D than for clay. D for sand is the same as for clay with $I_p = 0$ in Vucetic and Dobry (1991) and Darendeli (2001).

- High plasticity clay:
- Vucetic and Dobry (1991) give a smaller D than Darendeli (2001) at γ_{cy}>0.03%, smaller than Seed and Idriss (1970) mean curve and close to Seed and Idriss (1970) lower curve.
- NGI tests give a somewhat higher D than Vucetic and Dobry (1991), but smaller than Darendeli (2001) and Seed and Idriss (1970) mean curve. NGI tests give D close to Seed and Idriss (1970) lower curve.
- NGI tests give a small effect of N, as in the literature correlations.

Low plasticity clay:

- Vucetic and Dobry (1991), Darendeli (2001) and Seed and Idriss (1970) mean curve give similar D for γ_{cy}>0.1%, but Darendeli (2001) gives lower D than the others for γ_{cy}<0.1%.
- NGI tests give significant effect of N with highest D for low N. This is not captured by the literature correlations.
- NGI tests are similar to Vucetic and Dobry (1991) and Seed and Idriss (1970) mean curve for γ_{cy}<0.1%, and higher than Darendeli (2001), especially at low γ_{cy}.

Sand:

- The literature correlations give D independent of D_r and a small effect of N.
- Vucetic and Dobry (1991) and Seed and Idriss (1970) mean curves are similar.
- Darendeli (2001) gives a lower D which is similar to Seed and Idriss (1970) lower curve.
- The NGI tests indicate that D depends significantly on N, but also on FC and D_r. This is in contradiction with the literature correlations.
- Darendeli (2001) predicts no effect of overconsolidation ratio, which agrees with only a small tendency for D to decrease with increasing overconsolidation ratio in the NGI tests.

Clean dense sand:

- NGI tests give D for N = 1 similar to Vucetic and Dobry (1991) and Seed and Idriss (1970) mean curve and is higher than Darendeli (2001). However, D decreases with N in the NGI tests, and the NGI tests give lower D than Vucetic and Dobry (1991) and Seed and Idriss (1970) mean curve when N > 1. The effect of N is more important for Dr = 80% than for Dr = 100%.

Dense sand with 20% fines:

- NGI tests give lower D than Vucetic and Dobry (1991) and Seed and Idriss (1970) mean curve and is similar to Darendeli (2001) for N = 1. However, D decreases with N in the NGI tests, and the NGI tests give even lower D than Darendeli (2001) when N > 1. The effect of N is more important for Dr = 100% than for Dr = 80%.

11.4. Summary and recommendations

There can be significant differences between D from the different literature sources. The agreement with the NGI tests varies from one case to the other, and the NGI tests do not clearly support one source in favour of the others. It is recommended to use the NGI curves for the different soil types in Figs. 5 and 6 with some engineering judgement as best estimate D. One may consider using D from the lowest correlation as a conservative estimate.

12. Discussion

The cyclic contour diagrams for sand and silt in the data base are generally based on predominantly silica soils, a coefficient of uniformity less than about $C_u = 12$, $D_{60} < 0.2$ mm, a load period of 10s, and a modest preshearing of 400 cycles with a cyclic shear stress of 4% of the vertical consolidation stress. Yang et al. (2022) showed that the contours did not seem to be significantly influenced by mineralogy when about half of the quartz content was replaced by K-Feldspar and Plagioclase, but the coefficient of uniformity and D_{60} could influence both the undrained static and cyclic shear strengths.

For sand and silt the relative density and the water content are used as a basis to select cyclic contour diagrams. The relative density is also used to select additional parameters for sand, such as φ'_p and α'. Relative density in situ is often estimated from cone penetration test (CPT) correlations according to e.g. Jamiolkowski et al. (2003). Estimating D_r from laboratory testing is subject to the determination of minimum and maximum dry densities. Both the in situ and the laboratory determination of D_r involve uncertainty. The water content is a simpler parameter, but reliable in situ measurements can be a challenge, especially in sand. The data base in Andersen (2015) offers the advantage of comparing the D_r-based estimate of parameters with a parallel estimation based on the water content. Potential differences in parameters determined based on D_r and water content should be evaluated based on engineering judgment. One should also keep in mind the scatter in the data that the correlations are based on.

Andersen (2015) includes diagrams that can be used to estimate corrections for load period and level of preshearing. Modest preshearing will normally cause increased strength and stiffness, but it should be noted that laboratory tests show that preshearing can cause degradation of strength and stiffness of overconsolidated soils (e.g. Andersen, 2015). This may not be a problem for the soil beneath a foundation since the soil beneath the foundation will be strengthened by the simultaneous increase in effective stresses from the weight of the platform The consolidation under the weight of the structure will also reduce the OCR prior to the design event and thus the potential for negative preshearing effect. Outside the platform, however, there may not be increased effective stresses, neither in clay or in sand, and the OCR may remain high. This can lead to a reduction in strength and stiffnesses outside the foundation, increasing with time.

Foundation design is often based on strength and stiffnesses from DSS tests, assuming that DSS data represent a reasonable average of triaxial compression, DSS and triaxial extension data. This may not always be true, especially for dense silt and sand, as discussed in Section 7.2. DSS testing requires less soil material, and time and costs are saved by limiting testing to DSS. The anisotropy data presented herein can be used to estimate the effect of anisotropy and whether it will be worth the extra effort to include monotonic and cyclic triaxial tests.

13. Summary and conclusions

The soil parameters needed to perform a foundation design of an offshore or a nearshore structure under cyclic loading from wind and/or waves can be estimated from an available data base. This includes cyclic shear strength, deformation parameters, pore pressure generation due to cyclic loading, initial shear modulus, consolidation characteristics, effective stress strength parameters, φ_p' and α' and damping.

The input to the data base are conventional parameters, like undrained static shear strength, plasticity index and overconsolidation ratio for clays, and relative density and/or water content, fines content and overconsolidation ratio for sand and silt.

The data base includes correlations and parameters from triaxial compression, direct simple shear and triaxial extension tests, for both static and cyclic loading, thus covering the typical stress-paths that

characterize different types of soil-foundation interaction behaviour. Therefore, the parameters are valid for a wide range of foundations, including skirted foundations, monopiles, gravity bases, jack-ups, suction anchors and piles. The data base does not include damping. Interpretation and guidance on damping parameters are therefore included in this paper.

The estimated soil parameters can be used in feasibility analyses before site-specific parameters are available and to reduce the amount of site-specific advanced laboratory testing in the final design phase. Furthermore, the procedure illustrated can serve as a guide to design the specifics of site-specific cyclic laboratory testing.

The application of the data base is demonstrated by examples for clay and for sand with different fines content.

CRediT authorship contribution statement

Knut H. Andersen: Writing – original draft, Prepared the manuscript. **Harun Kursat Engin:** Writing – review & editing, Reviewed the manuscript. **Marco D'Ignazio:** Writing – review & editing, Reviewed the manuscript. **Shaoli Yang:** Writing – review & editing, Reviewed the manuscript.

Declaration of competing interest

The authors declare that they have no known competing financial interests or personal relationships that could have appeared to influence the work reported in this paper.

Data availability

Data is available in the referenced publications.

Acknowledgement

The discussions with colleagues at NGI in the development and use of the procedures described herein, as well as the support from NGI, is gratefully acknowledged.

The authors also acknowledge partial support from the project "Reducing cost of offshore wind by integrated structural and geotechnical design 2 (REDWIN 2)" funded by the Norwegian Research Council under the grant 296511.

References

Andersen, K.H., 2004. Cyclic clay data for foundation design of structures subjected to wave loading. General Lecture. In: Proc., Intern. Conf. On Cyclic Behaviour of Soils and Liquefaction Phenomena, CBS04, Bochum, Germany, 31.3-2.4, 2004. Proc. A.A. Balkema Publishers, Triantafyllidis, pp. 371–387. Th.

Andersen, K.H., 2015. Cyclic soil parameters for offshore foundation design. 3rd ISSMGE McClelland Lecture. In: Frontiers in Offshore Geotechnics III, ISFOG'2015, Meyer. Taylor & Francis Group, London, 978-1-138-02848-7. Proc., 5-82. Rev. version in: http://www.issmge.org/committees/technical-committees/applications/offshore and click on "Additional Information".

Andersen, K.H., Berre, T., 1999. Behaviour of a dense sand under monotonic and cyclic loading. In: Geotechnical Engineering for Transportation Infrastructure. 12th ECSGE Amsterdam, The Netherlands. Proc, vol. 2. Publ. by A.A. Balkema, pp. 667–676.

Andersen, K.H., Jostad, H.P., 1999. Foundation design of skirted foundations and anchors in clay. In: Proc. Offshore Technology Conference. Paper 10824, Houston, USA.

Andersen, K.H., Kleven, A., Heien, D., 1988b. Cyclic soil data for design of gravity structures. ASCE J. of Geotech. Engrg. 114 (5), 517–539.

Andersen, K.H., Lauritzsen, R., 1988a. Bearing capacity for foundation with cyclic loads. ASCE J. of Geotech. Engrg. 114 (5), 540–555.

Andersen, K.H., Schjetne, K., 2013. Data base of friction angles of sand and consolidation characteristics of sand, silt and clay. ASCE J. of Geotech. and Env. Engrg. 139 (7), 1140–1155.

Andersen, K.H., Dyvik, R., Lauritzsen, R., Heien, D., Hårvik, L., Amundsen, T., 1989. Model tests of offshore platforms. II. Interpretation. ASCE J. of Geotech. Engrg. 115 (11), 1550–1568.

Andersen, K.H., Dyvik, R., Schrøder, K., Bysveen, S., 1993. Field tests of anchors in clay. II: prediction and interpretation. ASCE J. of Geotech. Engrg. 119 (10), 1532–1549.

Andersen, K.H., Murff, J.D., Randolph, M.F., Clukey, E.C., Erbrich, C.T., Jostad, H.P., Hansen, B., Aubeny, C., Sharma, P., Supachawarote, C., 2005. Suction anchors for deepwater applications. In: Proc. 1st International Symposium on Frontiers in Offshore Geotechnics. ISFOG, Perth, pp. 3–30.

Andersen, K.H., Jostad, H.P., Dyvik, R., 2008. Penetration resistance of offshore skirted foundation and anchors in sand. ASCE J. of Geotech. and Geoenv. Engrg. (JGGE) 134 (1), 106–116.

Andersen, K.H., Puech, A., Jardine, R., 2013. Cyclic resistant geotechnical design and parameter selection for offshore engineering and other applications. In: Keynote Lecture. XVIIIth ICSMGE, TC209 Workshop – Design for Cyclic Loading; Piles and Other Foundations, Proc. Paris, 4. Sept. 2013.

Blaker, Ø., Andersen, K.H., 2015. Shear strength of dense to very dense Dogger Bank sand. In: Frontiers in Offshore Geotechnics III, ISFOG'2015, Meyer. Taylor & Francis Group, London, pp. 1167–1172, 978-1-138-02848-7. Proc.

Blaker, Ø., Andersen, K.H., 2019. Cyclic properties of dense to very dense silica sand. Soils Found. 59 (2019), 982–1000. https://doi.org/10.1016/j.sandf.2019.04.002.

Colreavy, C., Boylan, N., Andersen, K.H., Huang, N.N., Girsang, C.H., 2022. Cyclic Behaviour of a Malaysian Deepwater Clay. OTC Asia. Paper OTC-31518-MS.

Darendeli, M.B., 2001. Development of a New Family of Normalized Modulus Reduction and Material Damping Curves. Ph.D. dissertation. Univ. of Texas, Austin. Aug. 2001.

Engin, H.K., Andersen, K.H., Jostad, H.P., 2021. Qualitative Assessment of Uncertainties in Estimation and Modelling of Cyclic Design Parameters, and the Consequences on Calculated Spud-Can Foundation Capacity and Stiffnesses of Jack-Up Platforms. Jack-up Forum, London, 2021.

Finnie, I.M.S., Hospers, B., Nowacki, F., Andersen, K.H., Kalsnes, B., 1999. Cyclic simple shear behaviour of a carbonate sand. In: Balkema, Al-Shafei (Ed.), 2nd Int. Conf. On Engrg. for Calcareous Sediments, Bahrain. Proc, vol. 1, pp. 87–100. Rotterdam, ISBN 90 5809 037X.

Hardin, B.O., Drnevich, V.P., 1970. Shear modulus and damping in soils: I. Measurements and parameter effects, II. Design equations and curves. Technical Reports UKY 27-70-CE 2 and 3. College of Engineering, University of Kentucky, Lexington, Kentucky. July 1970.

Hardin, B.O., Drnevich, V.P., 1972. Shear modulus and damping in soils: design equations and curves. ASCE J. of Geotech. Engrg., Geotechnical Special Pub. 98 (118).

He, B., Yang, S., Andersen, K.H., 2021. Soil parameters for offshore windfarm foundation design: a case study of Zhuanghe wind farm. Eng. Geol. 285 (2021), 106055.

Idriss, I.M., 1990. Response of soft soil sites during earthquakes. In: Proc., H. Bolton Memorial Symp., vol. 2, pp. 273–289.

Jamiolkowski, M.B., Lo Presti, D.C.F., Manassero, M., 2003. Evaluation of Relative Density and Shear Strength of Sands from CPT and DMT, vol. 119. Soil Behavior and Soft Ground Construction, ASCE, GSP, pp. 201–238.

Jeanjean, P., Andersen, K.H., Kalsnes, B., 1998. Soil Parameters for Design of Suction Caissons for Gulf of Mexico Deepwater Clays. OTC, Houston. Proc., Paper 8830.

Jostad, H.P., Andersen, K.H., 2015. Calculation of Undrained Holding Capacity of Suction Anchors in Clay. Frontiers in Offshore Geotechnics III, ISFOG'2015, Meyer. Taylor & Francis Group, London, pp. 263–268. ISBN: 978-1-138-02848-7. Proc.

Jostad, H.P., Grimstad, G., Andersen, K.H., Saue, M., Shin, Y., You, D., 2014. A FE procedure for foundation design of offshore structures – applied to study a potential OWT monopile foundation in the Korean Western Sea. Geotech. Engrg. J. of the SEAGS & AGSSEA 45 (4). Dec. 2014.

Jostad, H.P., Grimstad, G., Andersen, K.H., Sivasithamparam, N., 2015. A FE Procedure for Calculation of Cyclic Behavior of Offshore Foundations under Partly Drained Conditions. ISFOG'2015, Meyer (Ed). Taylor & Francis Group, London, pp. 153–172. ISBN: 978-1-138-02848-7. Proc.

Kleven, A., Andersen, K.H., 1991. Cyclic laboratory tests on storebælt clay till. Seminar on design of exposed bridge piers. In: Danish Soc. Of Hydr. Engrg. Copenhagen, Denmark, 22 Jan. 1991. Also published in NGI Publ. 199.

Liedtke, E., Andersen, K.H., Zhang, Y., Jeanjean, P., 2019. Monotonic and Cyclic Soil Properties of Gulf of Mexico Clays. Offsh. Techn. Conf., Houston, Texas. OTC-29622.

Liu, D., Liu, B., Zhang, Y., Ma, Z., Andersen, K.H., Jostad, H.P., Li, L., Zhang, Y., 2020a. Long-term settlement of suction caisson foundations supporting offshore wind turbines. In: 30th Intern. Ocean and Polar Engrg. Conf. ISOPE, Shanghai, 2020.

Liu, B., Zhang, Y., Ma, Z., Andersen, K.H., Jostad, H.P., Liu, D., Pei, A., 2020b. Design considerations of suction caisson foundations for offshore wind turbines in Southern China. Appl. Ocean Res. 104, 102358 https://doi.org/10.1016/j.apor.2020.102358.

Løvholt, F., Madshus, C., Andersen, K.H., 2020. Intrinsic soil damping from cyclic laboratory tests with average strain development. Geotech. Test J. 43 (1), 20170411 https://doi.org/10.1520/GTJ20170411. Available online at: www.astm.org.

Lunne, T., Andersen, K.H., 2007. Soft clay shear strength parameters for deepwater geotechnical design. In: Keynote; Proc., 6th Intern. Offsh. Site Investigation and Geotechnics Conf.; Confronting New Challenges and Sharing Knowledge, 151-176, 11-13 September 2007 (London, UK).

Seed, H.B., Idriss, I.M., 1970. Soil Moduli and Damping Factors for Dynamic Response Analyses. Earthquake Engrg. Research Center. Rep. No. EERC 70-10, Dec. 1979.

Seed, H.B., Wong, R.T., Idriss, I.M., Tokimatsu, K., 1986. Moduli and damping factors for dynamic analyses of cohesionless soils. ASCE, JSMFD 112 (11), 1016–1032.

Sun, J.I., Golesorkhi, R., Seed, H.B., 1988. Dynamic Moduli and Damping Ratios for Cohesive Soils, p. 48. Rep., UCB/EERC-88-15, UC Berkely.

Vucetic, M., Dobry, R., 1991. Effect of soil plasticity on cyclic response. ASCE, JGE 117 (1), 89–107.
Wichtmann, T., Andersen, K.H., Sjursen, M.A., Berre, T., 2013. Cyclic tests on high-quality undisturbed block samples of soft marine Norwegian clay. Can. Geotech. J. 50 (2013), 400–412. https://doi.org/10.1139/cgj-2011-0390.
Yang, S., He, B., Andersen, K.H., Firouzianbandpey, S., 2022. Monotonic and Cyclic Properties of Silty Sand and Sandy Silt for Foundation Design of Offshore Windfarms (Accepted for publ. in Canadian Geotechnical Journal).

List of Symbols and Abbreviations

C_u: Coefficient of uniformity, $C_u = D_{60}/D_{10}$
D: Damping ratio
D_r: Relative density
D_{10}: Particle diameter where 10% of the population is smaller
D_{60}: Particle diameter where 60% of the population is smaller
DSS: Direct simple shear
FC: Fines content
F_{Ip}: Correction factor for plasticity on cyclic shear stress at failure
$F_{Ip\ small\ strain}$: Correction factor for plasticity on G_{max}
$F_{Ip\ 50\%}$: Correction factor for plasticity on shear modulus at 50% of failure
G_{max}: Initial shear modulus
I_p: Plasticity index
M: Constrained modulus, tangent
m: Exponent in SHANSEP equation
N: Number of cycles
NC: Normally consolidated
N_{eq}: Number of maximum load cycles that is equivalent to the full load history
N_f: Number of cycles to failure
NGI: Norwegian Geotechnical Institute
OC: Overconsolidated
OCR: Overconsolidation ratio
P: Load
p: Exponent in equation for G as function of OCR
s_{uD}, s_{uC}, s_{uE}: Undrained shear strength in DSS, triaxial compression and triaxial extension, respectively
u_p: Permanent pore pressure (pore pressure at end of a cycle)
w: Water content
α': Slope of failure line in DSS effective stress path plot
φ_p': Peak drained friction angle
γ_a, γ_{cy}: Average and cyclic shear strain, respectively
σ'_{vc}: Vertical effective stress
σ'_{ref}: Reference stress, $\sigma'_{ref} = p_a \cdot (\sigma'_{vc}/p_a)^n$, where p_a is the atmospheric pressure (=100 kP), and exponent n is a function of normalized undrained shear strength of the soil in its normally consolidated state
τ_0: Initial shear stress
τ_a, τ_{cy}: Average and cyclic shear stress, respectively
$\tau_{a,f}$, $\tau_{cy,f}$: Average and cyclic shear stress components at failure, respectively
τ_f: Shear stress at failure
$\tau_{f,cy}$: Cyclic shear stress at failure, $\tau_{f,cy} = \tau_{a,f} + \tau_{cy,f}$